A laser-driven undulator x-ray source: simulation of image formation and dose deposition in mammography

Bernhard Müller^{1,2}, Helmut Schlattl², Florian Grüner¹, Christoph Hoeschen²

ABSTRACT

Since overcoming some of the inherent limitations of x-ray tubes becomes increasingly harder, it is important to consider new ways of x-ray generation and to study their applications in the field of medical imaging. In the present work we investigate a novel table-top-sized x-ray source, developed in a joint project within the Cluster of Excellence "Munich Center for Advanced Photonics". It uses laser-accelerated electrons emitting x-ray radiation in a short period undulator. This source has the potential to deliver tunable x-rays with a very narrow spectral bandwidth. The main purpose of this contribution is to investigate the performance of this source in the field of mammography and to compare it to that of conventional x-ray tubes. We simulated the whole imaging process from the electron beam dynamics through the generation of the synchrotron radiation in the undulator up to the x-ray-matter interaction and detection in the mammographic setting. A Monte Carlo simulation of the absorption and scattering processes based on the Geant4 software toolkit has been developed that uses a high-resolution voxel phantom of the female breast for the accurate simulation of mammography. We present simulated mammograms generated by using quasi-monochromatic undulator radiation and by using the polychromatic spectrum of a conventional x-ray tube.

Keywords: x-ray source, laser-driven, quasi-monochromatic spectrum, mammography, Geant4 simulation

1. INTRODUCTION

In todays radiological practice x-ray imaging is based on x-ray tubes. These, however, have some inherent deficiencies that are problematic to overcome. Among others the broad bremsstrahlung spectrum and the finite focal-spot size are worth mentioning. Especially in mammography where the differentiation between normal and cancerous tissue in x-ray absorption imaging ist very challenging and in the light of breast screening programs it is important to optimize the image-quality-to-dose relationship. It is known, that by K-edge filtration and by choosing the right x-ray tube parameters the x-ray spectrum can be optimized and the dose can be significantly lowered in mammography.¹⁻³ However even after K-edge filtration a considerable number of low energy photons remains and the filtration is limited by the resulting low fluence rate.

Therefore new ways of generating x-rays have to be investigated in order to improve the image-quality-to-dose relationship in mammography. At large kilometer-scale synchrotron facilities the use of synchrotron radiation in mammographic settings has been investigated and the advantages have been shown in experiments.^{4,5} In order to get comparable results with laboratory sized x-ray sources there have been developments like Thomson scattering sources which are based on Thomson back scattering of accelerated electrons with laser pulses.⁶

The system we investigated in this work is a table-top sized laser-driven x-ray source⁷ that allows the generation of tunable quasi-monochromatic x-rays. This source consists of a laser-driven electron accelerator and an undulator⁸ which is a periodic arrangement of magnets, that forces the electrons into an oscillating motion which makes them spontaneously emit synchrotron radiation. The electron acceleration is based on a laser-plasma acceleration scheme, ⁹⁻¹² together with an electron optic to focus the electron beam. First experiments with this source have already demonstrated the production of spontaneous undulator radiation in the soft x-ray range.⁷ Since it has already been shown that laser-plasma accelerators are capable of producing quasi-monochromatic

¹Department of Physics, Ludwig-Maximilians-Universität München, 85748 Garching, Germany

²Department of Medical Radiation Physics and Diagnostics, Helmholtz Zentrum München German Research Center for Environmental Health, 85764 Neuherberg, Germany

electrons at a few GeV, ^{13,14} it will be possible to reach higher x-ray energies suitable for medical imaging in the near future.

The experimental setup is depicted in Fig. 1 and consists of several parts. The electron acceleration is done by an intense laser pulse, which ionizes the atoms of a gas target and produces a plasma wave that generates large longitudinal electrical fields by which the electrons get accelerated to relativistic energies.¹² The electron optics part consists of two magnetic quadrupole lenses¹⁵ that ensure the collimation and focusing of the electron beam. Because, depending on their parameters, they focus only electrons of a specific energy they also act as energy-band-pass filter, which ensures a small spectral bandwidth and stability in terms of low shot-to-shot fluctuations.⁷ The x-rays are generated inside the undulator and result from the sinusoidal motion of the electrons caused by the magnetic field, thereby emitting synchrotron radiation in a narrow cone. Finally the electrons get deflected by a magnetic field onto a beam dump.

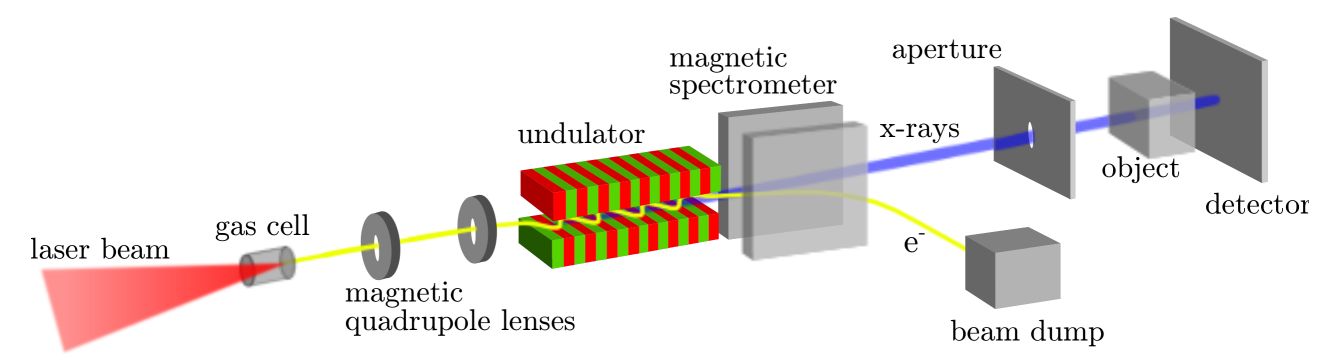


Figure 1. Experimental setup of the undulator radiation source.

The radiation produced by this setup depends on the different experimental parameters and has the following characteristic properties. The spectrum of the spontaneous undulator radiation consists of a peak at a fundamental energy and of higher energy photons of higher harmonic frequencies, which can be seen in Fig. 2.

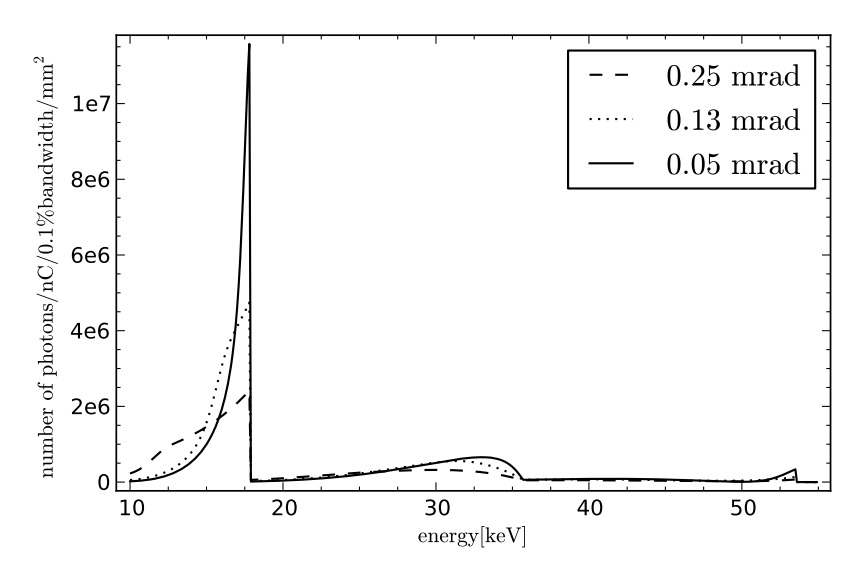


Figure 2. Spectral on-axis photon flux of the spontaneous undulator radiation produced by 3.3 GeV electrons plotted for different off-axis collection angles. The fundamental with a peak energy at about 18 keV and the second and third harmonic are shown.

The wavelength of the n-th harmonic is given by

$$\lambda_n = \frac{\lambda_u}{2\gamma^2 n} \left(1 + \frac{K^2}{2} + \gamma^2 \theta^2 \right) \tag{1}$$

where γ is the Lorentz factor of the electrons, θ is the off-axis observation angle and K ist the deflection parameter which is proportional to the undulator period λ_u and the amplitude of the undulators magnetic field strength B_0 .¹⁶ Consequently, the x-ray energy can be tuned with the electron energy which itself can be selected by choosing the corresponding quadrupole parameters, because of the band-pass property of the electron optic mentioned above. However, because of the relativistic doppler effect the discrete harmonic wavelengths possess a characteristic angular θ^2 dependency which can be seen in Fig. 4. This results in a broader total spectrum when collecting the beam at higher angles θ as shown in Fig. 2 and explains the neccessity of the beam aperture in order to achieve a high level of monochromaticity.

The relative on-axis ($\theta = 0$) bandwidth of the n-th harmonic (FWHM) is given by

$$\frac{\Delta E}{E_n} \approx \frac{2 \times 1.4}{\pi n N_u} \approx \frac{1}{n N_u} \tag{2}$$

where N_u is the number of undulator periods and $K \propto B_0 \lambda_u$ is the deflection parameter.¹⁶ Consequently for a high number of undulator periods we get a nearly monochromatic beam.

For an undulator with deflection parameter K < 1 the total number of photons in the central cone of the fundamental energy is approximately

$$N \approx 1.43 \times 10^{14} N_u Q_e \frac{K^2}{1 + \frac{K^2}{2}} \tag{3}$$

where Q_e is the charge of the electron bunch of the shot.¹⁶ When the laser is pulsed at high frequencies this will deliver a sufficient number of photons for imaging applications.

The average divergence of the radiation cones produced inside the undulator is given by

$$\theta_{\rm rms} \approx \frac{1}{2\gamma} \sqrt{\frac{1 + \frac{K^2}{2}}{nN_u}} \approx \frac{1}{2\gamma\sqrt{N_u}}$$
 (4)

This divergence of the radiation is the main factor for the resolution properties of the source, the smaller it is, the smaller are the details that can be resolved in the x-ray absorption image.

The purpose of the present work is to present a simulation of the image formation and dose deposition process using laser-driven undulator x-ray sources in mammographic absorption imaging. We show simulated mammograms of a voxelmodel of the breast using quasi-monochromatic undulator radiation and polychromatic x-ray tube spectra together with the calculated average glandular radiation dose.

2. MATERIALS AND METHODS

We calculated the electron beam dynamics as well as the generation of synchrotron radiation in the undulator using serveral well established software tools in order to get suitable working parameters of the source simulating mammographic absorption imaging. This allows us to evaluate the influence of the parameters of the source and of the detection geometry on the resulting image quality. A Monte Carlo simulation of the absorption and scattering processes has been written that utilizes the calculated x-ray beam and a high-resolution voxelmodel of the female breast 17 and provides information about the image formation and dose deposition process.

The beamline setup is depicted in Fig. 1 and consists of the magnetic quadrupoles that focus the electrons, the undulator and the detector. The imaging of the whole breast is done by sequentially imaging small parts, each imaged part corresponding to a shot of the source which is pulsed at a certain frequency.

2.1 Calculation of the x-ray beam

As basic starting parameters of the laser-accelerated electrons we used values from previous calculations that have been confirmed by experiments. These are an initial electron source distribution with a r.m.s. size of about 1 μ m, a normalized emittance of 1 mm mrad and an initial divergence of about 1 mrad. The magnetic quadrupoles both have a field gradient of 500 $\frac{T}{m}$ and an aperture diameter of 6 mm. The undulator is positioned after the second quadrupole and produces a sinusoidal field with a field strength amplitude of 1.2 T at a gap width of 1.2 mm and with 60 periods of length 5 mm. The resulting x-ray beam is collimated by an aperture with a diameter of 0.2 mm at a distance of about 4 m after the undulator exit.

To estimate the photon energy that optimizes the image quality to dose relation when imaging our voxel model that has a thickness of about 4 cm, we previously simulated mammograms with different monoenergetic photons and tube spectra. We found x-rays of about 18 keV to give the best image quality to dose relationship in terms of SDNR²/AGD where SDNR is the signal difference to noise ratio and AGD is the average glandular dose. It can be calculated from Eq. 1 that the electron energy which gives the optimal x-ray energy is about 3.3 GeV as this results in a fundamental energy peak at about 17.9 keV.

As described above, the magnetic quadrupoles are used to collect the accelerated electrons and to focus them. We had to find the parameters for the magnetic quadrupoles that delivers a beam that stays within the boundary parameters of the source like quadrupole aperture size and undulator gap size. By using the beam physics package of the code system $COSY^{18}$ we were able to find those parameters that conform with the systems boundaries.

We calculated the many particle electron dynamics by using the code GPT.¹⁹ Thereby we tracked the electrons through the magnetic quadrupole lenses and determined their position and momentum distribution along the longitudinal axis. The parameters of the magnetic quadrupoles and the resulting electron beam properties are shown in table 2.1 and the horizontal and vertical size of the electron bunch are plotted in Fig. 3.

Quad. Param.	position [m]	length [cm]	r.m.s. Beam size	size [mm]	divergence [mrad]
Quad. 1	0.990	4.35	vertical	0.445	12.5
Quad. 2	1.41	3.28	horizontal	2.00	55.6

Table 1. Magnetic Quadrupole parameters (left) leading to an electron beam with a small average bunch size in the undulator (right).

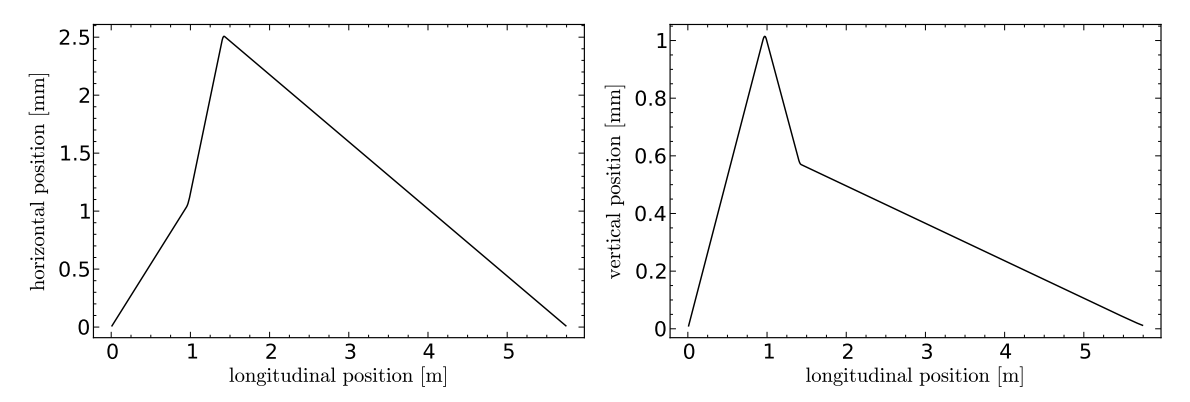


Figure 3. Horizontal (left) and vertical (right) r.m.s electron bunch sizes plotted against the longitudinal position in the beam line.

Because of the initial gaussian position and divergence distribution of the electrons, their distribution in phase space is also at all times a two dimensional gaussian that can be characterized by the standard deviations of position and momentum. As the electrons get focused by the quadrupoles and in free drift their distribution only

gets deformed, because of phase space volume conservation and can still be described by those two parameters. In order to efficiently calculate the undulator radiation, produced by this electron distribution we determined the phase space parameters of the electrons inside the undulator. The knowledge of those parameters enabled us to calculate the synchrotron radiation by using the well established algorithms of the code system SRW.²⁰ Appropriate routines for the efficient sampling of the x-ray production in the undulator in spatial and spectral domain and for determining the beam divergence and spatial distribution on the detector have been written using the algorithms of that code. We thereby calculated the synchrotron radiation cones produced at a finite number of $n_h \times n_v \times n_l$ points inside the undulator which provides the full information about the source size inside the undulator as well as the divergence of the radiation cones originating from those points and the spatial distribution of the x-rays in the detector plane as a function of the x-ray energy. The resulting beam profile in the detector plane is plotted in Fig. 4. In accordance with Eq. 3 the total number of photons in the spectrum was calculated to be 1.7×10^8 photons per nC electron charge.

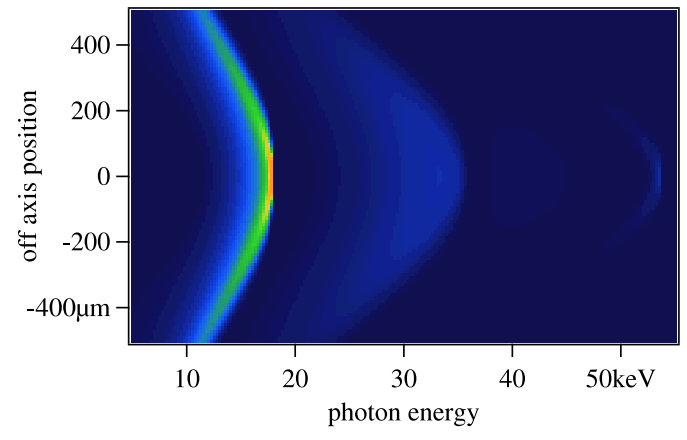


Figure 4. Spectral photon flux in the detector plane plotted against the photon energy and the off-axis position.

2.2 Monte Carlo simulation of mammographic x-ray absorption imaging

A Monte Carlo simulation has been written, based on the Geant4 software toolkit²¹ that reads the previously calculated undulator radiation beam and simulates the absorption and scattering processes in the mammographic setting. As the x-rays are produced by a gaussian-shaped electron phase-space distribution the resulting x-ray beam also has gaussian shape. We use that a-priori information about the beam in order to get a more accurate calculation and to eliminate sampling artifacts resulting from the finite number of sampling points $n_h \times n_v$ from the previous calculations. The simulation therefore employs a fitting routine that fits a two dimensional gaussian to the intensities of the radiation emitted from those $n_h \times n_v$ points for each energy. When the photons are generated in the simulation, we use the variances calculated by the fitting routine to get a smooth gaussian-shaped beam profile.

To model the setting of mammography as accurately as possible and to get realistic images the simulation uses a voxel-model of the breast that has been reconstructed from CT-scans of a human breast specimen and was segmented into skin tissue, glandular tissue and adipose tissue.¹⁷



Figure 5. Transversal and frontal section of the breast voxelmodel.

The composition of the different tissues was taken from the literature. 22 Together with that also more simple phantoms were used, to validate the simulation with the more complex voxel-phantom and for comparison with the literature. 2,3,6

The x-ray matter interaction is simulated by using either the Geant4 low energy or the PENELOPE physics model, taking into account Photo effect, Compton scattering and Rayleigh scattering. Only individual photons are processed without variance-reduction techniques or further approximations. The detector is assumed to be of an ideal energy integrating type i.e. with a DQE of 1 and a pixel size approximately 7 times smaller than the voxel size. The main output of the simulation are energy resolved images of the total (primary and scattered) x-ray energy on the detector. Fig. 7 shows a mammogram, simulated with the undulator radiation source.

The simulation of mammographic absorption imaging with x-ray tubes has also been done with the same Monte Carlo simulation, by using mammographic spectra found in the literature²³ and by using a r.m.s. focal spot size of about 1 mm at 1.5 m distance to the breast. To get a meaningful comparison of the undulator source with x-ray tubes, we used the x-ray spectrum that provided the best image quality to dose relationship in our setting. In accordance with the literature^{3,6} this was found to be the spectrum of a Molybdenum anode with 30 µm Molybdenum filter as shown in Fig. 6.

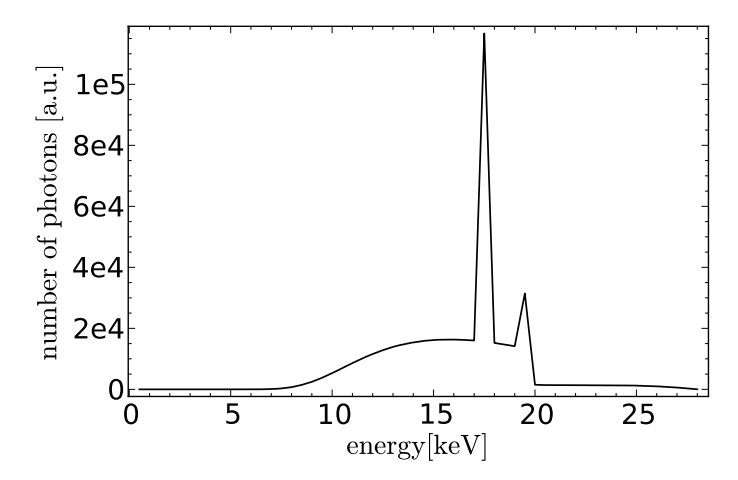


Figure 6. Spectrum of an x-ray tube with Molybdenum anode, at 28 kVp and 30 µm Molybdenum filter.

Alltogether, these procedures constitute a full start-to-end simulation of the x-ray production with an undulator x-ray source and its application to x-ray absorption imaging in mammography. Because of the accurate calculation of the synchrotron radiation, this allows us to not only compare the influence of the quasi-monochromatic spectrum on the image contrast but also to get information about the spatial resolution properties of the undulator x-ray source. As the simulation uses no further approximations or variance-reduction techniques the programme had to be parallelized on a cluster in order to generate a sufficiently large number of photons comparable to real mammograms.

3. RESULTS

We simulated mammographic absorption imaging using the x-ray undulator radiation generated by 3.3 GeV electrons. In this simulation the contribution of the higher harmonics in the spectrum has been neglected and only the fundamental at a collection angle of 0.05 mrad has been considered. The resulting mammogram is shown In Fig. 7. A magnified part of the whole mammogram is shown in Fig. 8 both for the mammogram simulated with the undulator x-ray source as well as for that simulated with the x-ray tube spectrum shown in Fig. 6, in order to illustrate the different image quality characteristics. A qualitative comparison of those parts already indicates, that the image simulated with the quasi-monochromatic undulator radiation possesses better contrast and noise properties.

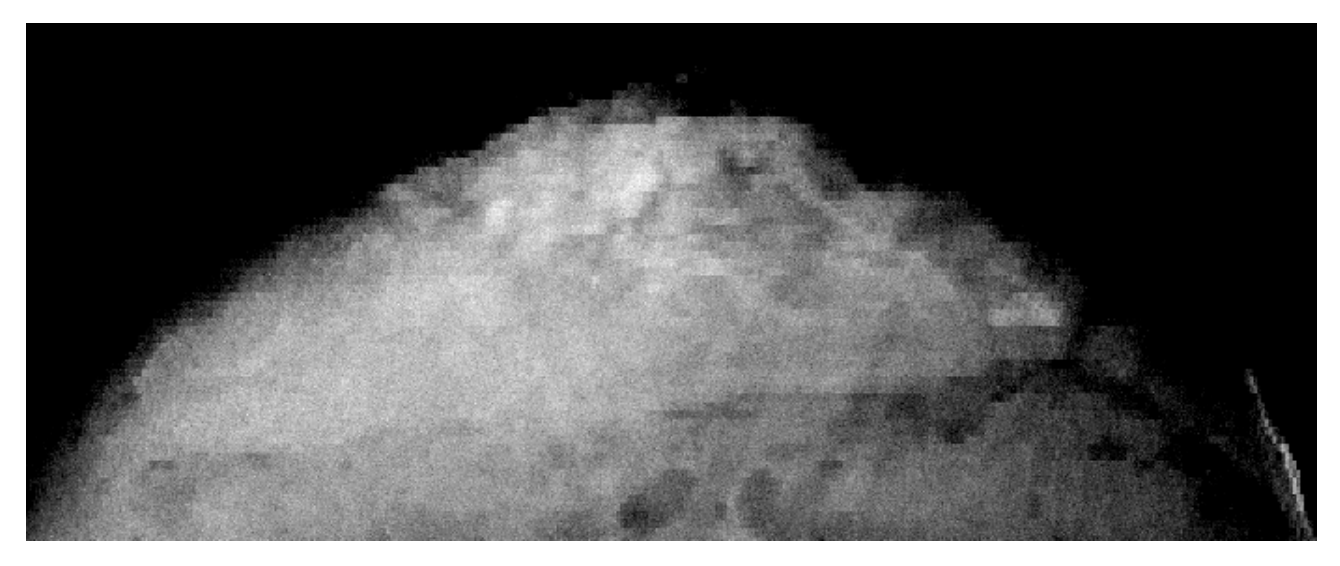
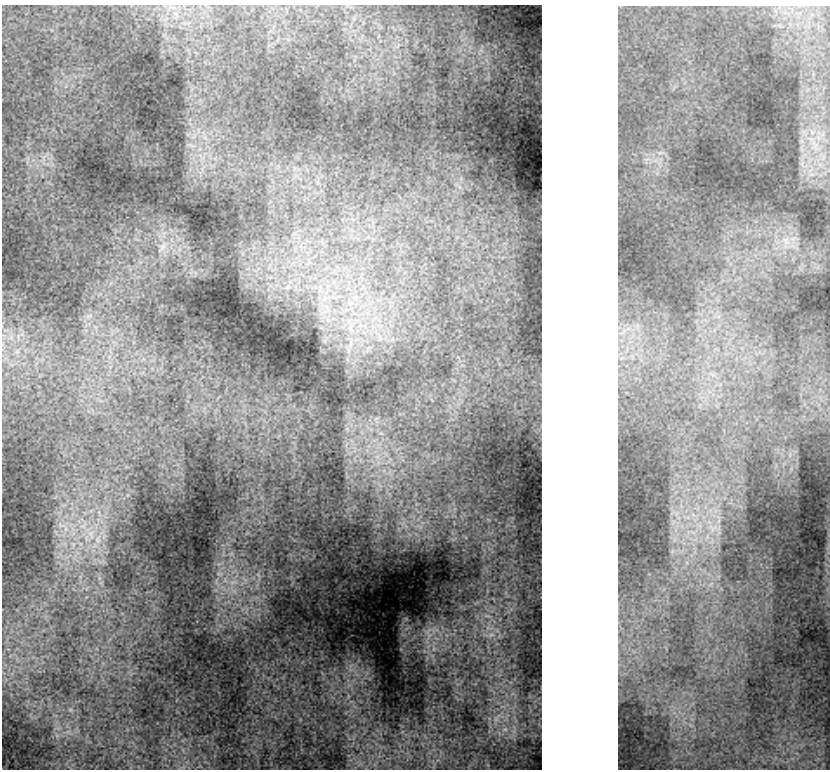


Figure 7. Detected total x-ray energy using quasi-monochromatic undulator radiation. The glandular dose deposited during the exposure is about 0.2 mGy at a total number of about 10^{11} incident photons. The simulation time was about one day on a cluster.



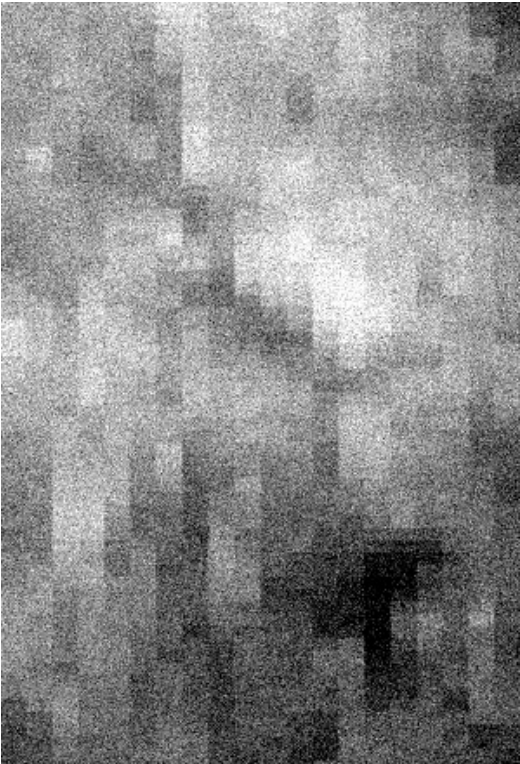


Figure 8. Magnified part of a mammogram simulated with a conventional x-ray tube (left) and of the mammogram shown in Fig. 7, simulated with the undulator radiation source (right).

In Fig. 9 we show the analysis of the spatial frequency of one edge detail, where it can be seen, that the image simulated with the undulator x-ray source contains higher frequencies when compared to the image simulated with the x-ray tube.

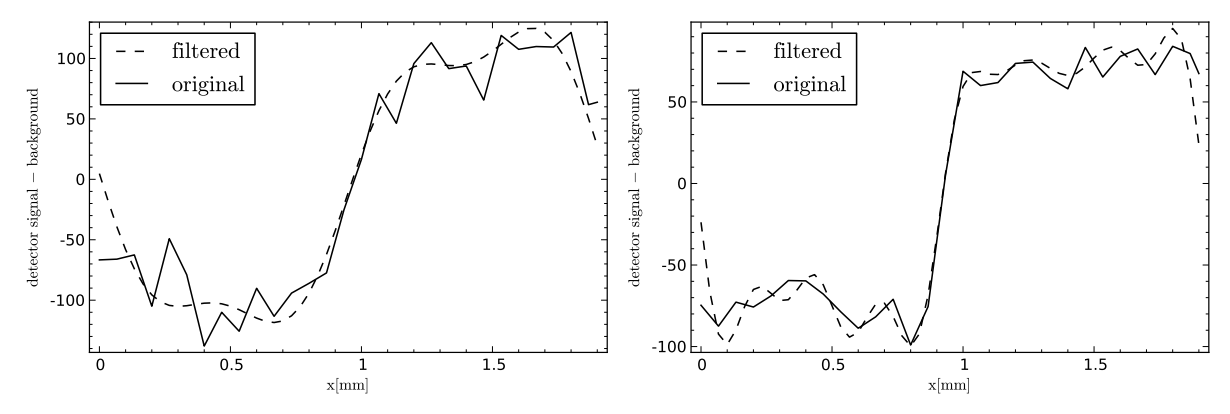


Figure 9. Integrated detector signal and low-pass filtered signal at a cut-off frequency of $1.5 \frac{1}{\text{mm}}$ of one ROI of the image simulated with the x-ray tube spectrum (left) and of the same ROI of the image simulated with the undulator x-ray source at a cut-off frequency of $4 \frac{1}{\text{mm}}$ (right).

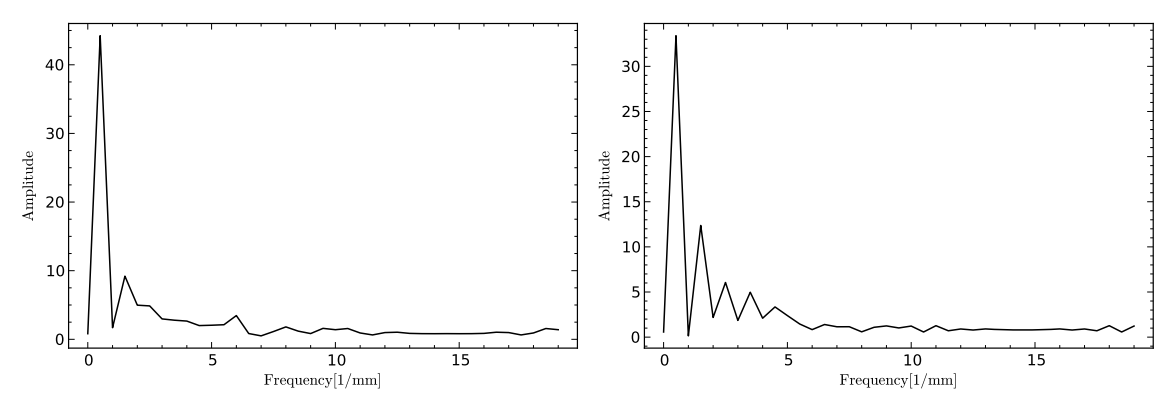


Figure 10. Amplitude spectrum of the detector signal shown in Fig. 9, of the image simulated with the x-ray tube spectrum (left) and of the corresponding detector signal in the image simulated with the x-ray undulator source (right).

4. DISCUSSION AND CONCLUSIONS

We presented the simulation of mammographic absorption imaging with a quasi-monochromatic x-ray source and the resulting mammograms. In this work, the high energy photons of the higher harmonics in the undulator spectrum have been neglegted, which would slightly increase the noise in the image. Note also that we used a tube spectrum that is highly optimized for our situation. But for thicker or denser breasts it might not be possible to find a tube spectrum that is that optimal while the undulator spectrum is continuously tunable. In this work we focused on obtaining an x-ray beam that is quasi monochromatic but it may as well be possible to make use of the energy-angle dependence seen in Fig. 4 in order to do dual energy imaging. However the setup investigated in this work is producing an x-ray beam profile that is not suitable for imaging larger areas needed in mammography. Even if the laser driving the source is pulsed at frequencies in the range of kHz it would take several minutes to image the whole breast. This shortcoming has to be addressed in future studies. The voxel-model we used had a voxel size of 0.5 mm, which we are planning to improve in future studies in order to quantify the image quality characteristics.

ACKNOWLEDGMENTS

This work was supported by the DFG Cluster of Excellence "Munich-Center for Advanced Photonics" (MAP).

REFERENCES

- [1] Thilander-Klang, A. C., Ackerholm, P. H. R., Berlin, I. C., N. G. Bjustam, S. L. J. M., Maanson, L. G., von Scheele, C., and Thunberg, S. J., "Influence of anode-filter combinations on image quality and radiation dose in 965 women undergoing mammography," *Radiology* 203, 348–354 (1997).
- [2] Dance, D. R., Thilander-Klang, A., Sandborg, M., Skinner, C. L., Smith, A. C., and Carlsson, G. A., "Influence of anode/filter material and tube potential on contrast, signal-to-noise ratio and average absorbed dose in mammography: A monte-carlo study," Br. J. Radiol. 73, 1056–1067 (1997).
- [3] Bernhardt, P., Mertelmeier, T., and Hoheisel, M., "X-ray spectrum optimization of full-field digital mammography: Simulation and phantom study," *Med. Phys.* **33**, 4337 (2006).
- [4] Moeckli, R., Verdun, F. R., Fiedler, S., Pachoud, M., Bulling, S., Schnyder, P., and Valley, J. F., "Influence of scatter reduction method and monochromatic beams on image quality and dose in mammography," *Med. Phys.* **30**, 3156–3164 (2003).
- [5] Moeckli, R., Verdun, F. R., Fiedler, S., Pachoud, M., Schnyder, P., and Valley, J. F., "Objective comparison of image quality and dose between conventional and synchrotron radiation mammography," *Phys. Med. Biol.* 45, 3509–3523 (2000).
- [6] Oliva, P., Golosio, P., Stumbo, S., Bravin, A., and Tomassini, P., "Compact x-ray sources for mammographic applications: Monte carlo simulations of image quality," *Med. Phys.* **36**, 5149 (2009).
- [7] Fuchs, M., Weingartner, R., Popp, A., Major, Z., Becker, S., Osterhoff, J., Cortrie, I., Zeitler, B., Hörlein, R., Tsakiris, G. D., Schramm, U., Rowlands-Rees, T. P., Hooker, S. M., Habs, D., Krausz, F., Karsch, S., and Grüner, F., "Laser-driven soft-x-ray undulator source," *Nature Physics* 5 (2009).
- [8] O'Shea, F. H., Marcus, G., Rosenzweig, J. B., Scheer, M., Bahrdt, J., Weingartner, R., Gaupp2, A., and Grüner, F., "Short period, high field cryogenic undulator for extreme performance x-ray free electron lasers," *Phys. Rev. ST Accel. Beams* 13, 070702 (2010).
- [9] Mangles, S. P. D. et al., "Monoenergetic beams of relativistic electrons from intense laser plasma interactions," *Nature* **431**, 535–538 (2004).
- [10] Geddes, C. G. R. et al., "High quality electron beams form a laser wakefield accelerator using plasma-channel guiding," *Nature* **431**, 538–541 (2004).
- [11] Faure, J. et al., "A laser-plasma accelerator producing monoenergetic electron beams," *Nature* **431**, 541–544 (2004).
- [12] Pukhov, A. and Meyer-ter Vehn, J., "Laser wake field acceleration: The highly non-linear broken-wave regime," Appl. Phys. B: Lasers Opt. 74, 355–361 (2002).
- [13] Osterhoff, J., Popp, A., Major, Z., Marx, B., Rowlands-Rees, T. P., Fuchs, M., Geissler, M., Hörlein, R., Hidding, B., Becker, S., Peralta, E. A., Schramm, U., Grüner, F., Habs, D., Krausz, F., Hooker, S. M., and Karsch, S., "Generation of stable, low-divergence electron beams by laser-wakefield acceleration in a steady-state-flow gas cell," *Phys. Rev. Lett.* **101**, 085002 (2008).
- [14] Hafz, N. A. M. et al., "Stable generation of gev-class electron beams from self-guided laser-plasma channels," *Nature Photon.* 2, 571–577 (2008).
- [15] Eichner, T., Grüner, F., Becker, S., Fuchs, M., Habs, D., Weingartner, R., Schramm, U., Backe, H., Kunz, P., and Lauth, W., "Miniature magnetic devices for laser-based, table-top free-electron lasers," *Phys. Rev. ST Accel. Beams* 10, 082401 (2007).
- [16] Clarke, J. A., [The Science and Technology of Undulators and Wigglers], Oxford Univ. Press (2004).
- [17] Hoeschen, C., Fill, U., Zankl, M., Panzer, W., Regulla, D., and Döhring, W., "A high-resolution voxel phantom of the breast for dose calculations in mammography," *Radiation Protection Dosimetry* **114**, 406–409 (2005).
- [18] Makino, K. and Berz, M., "Cosy infinity version 8," Nuclear Instruments and Methods in Physics Research A 427, 338–343 (1999).

Proc. of SPIE Vol. 7961 796106-9

- [19] van der Geer, S. and de Loos, M., "General particle tracer: A 3d code for accelerator and beamline design," *Proc. EPA C98*, 1245 (1998).
- [20] Chubar, O. and Elleaume, P., "Accurate and efficient computation of synchrotron radiation in the near field region," *Proc. EPAC98*, 1177–1179 (1998).
- [21] Agostinelli, S. et al., "Geant4: a simulation toolkit," Nuclear Instruments and Methods in Physics Research A 506, 250–303 (2003).
- [22] ICRU, "Tissue substitutes in radiation dosimetry and measurement," ICRU Report 44 (1989).
- [23] Cranley, K., Gilmore, B., Fogarty, G., and Desponds, L., "Catalogue of diagnostic x-ray spectra and other data," *IPEM Report* 78 (1997).